Polymer Journal (2015) 47, 428–433

www.nature.com/pj

ORIGINAL ARTICLE

Dynamic light scattering study of the curing mechanisms of novolac-type phenolic resins

Yasuyuki Shudo[1,2], Atsushi Izumi[2], Takeshi Takeuchi[2], Toshio Nakao[1] and Mitsuhiro Shibayama[1]

The curing behavior of a novolac resin (NV) cured with hexamethylenetetramine (HMTA), as well as the influence of an excess amount of HMTA on the curing reaction, were investigated by dynamic light scattering and gel permeation chromatography. A two-roll mixing mill process was applied to control the curing reaction degree. The dependence of the number of mixing times on the weight-average molecular weight (M_w) and hydrodynamic radius (R_h) of NV differed significantly with the HMTA amount. A larger quantity of HMTA resulted in faster growth and larger R_h and M_w values. The relationship between M_w and R_h for NV in tetrahydrofuran indicates two different polymer-growth mechanisms irrespective of the excess amount of HMTA (that is, power-law and subsequent deviation corresponding to the chain extension and intermolecular reactions between larger molecules, respectively). These results suggest that structural differences governing the mechanical properties of phenolic resins are initiated in the pregel stage, followed by noticeable differences in the mechanical properties during the subsequent curing process.
Polymer Journal (2015) **47,** 428–433; doi:10.1038/pj.2015.15; published online 18 March 2015

INTRODUCTION

Phenolic resins, which are well-known phenol formaldehyde resins or Bakelite, were invented by Baekeland in 1907 and employed as the first commercial synthetic polymer.[1] These polymers have been used as indispensable thermosetting resins in the electronic, automotive, aerospace, housing and other industries due to their excellent mechanical and electrical properties, as well as their resistance to heat and solvent.[2–4]

For general industrial use, cured phenolic resins are prepared by curing a novolac-type phenolic resin oligomer (NV) with hexamethylenetetramine (HMTA) as the curing agent (Figure 1). NV can be obtained via the polycondensation of phenol and formaldehyde in the presence of an acid catalyst, such as oxalic acid.[2] For phenolic resins, the degree of the reaction (α) is defined as the fraction of reacted *ortho*- and *para*-positions adjacent to hydroxyl groups and is based on classical gelation theory.[5–7] NV are further heat treated in the presence of HMTA to obtain cured phenolic resins. Therefore, understanding and controlling the chemical structure and curing behavior of these resins are important. Several studies have been performed on NV using infrared (IR)[8] spectroscopy, nuclear magnetic resonance (NMR)[9–11] spectroscopy and differential scanning calorimetry.[12–14]

The excellent properties of cured phenolic resins are derived from their three-dimensional, cross-linked network structures, as well as their high crosslink densities. To obtain highly cured phenolic resins, an excess amount of HMTA (greater than the stoichiometric ratio) is frequently used for industrial curing of NV.[2,3] Experimentally, the preparation of phenolic resins with an excess amount of HMTA results in an improvement in the mechanical strength and modulus of the cured resins. However, the influence of the excess amounts of HMTA on the resulting cross-linked structure has not been well studied owing to challenges associated with analyzing the structures of insoluble and infusible cured phenolic resins.

The main objective of the current study was to elucidate the relationship between the mechanical properties and network structure of phenolic resins. Previously, we investigated the inhomogeneity of phenolic resins using dynamic light scattering (DLS), small-angle X-ray (SAXS) and neutron scattering (SANS) and molecular dynamics simulations.[15–20] These scattering techniques are powerful tools for elucidating the inhomogeneity of cross-linked materials, including soluble oligomers, insoluble gels and infusible cured resins.[21–24] However, studies of phenolic resins using scattering techniques have been limited to polymer blends[25] and composite materials[26] with phenolic resins except for our previous studies.[16–20] In our previous studies, conformational analysis was performed in the solution state, which was achieved by dissolving bulk reaction mixtures into good solvents, using DLS to gain insight into the phenol–formaldehyde polycondensation mechanism below the gel point.[16] Well below the gel point, phenolic resins exhibit self-similar structures with respect to their molecular weights, which results in a power-law relationship between the hydrodynamic radius (R_h) and the weight-average molecular weight (M_w). We also carried out SAXS and SANS

[1]Neutron Science Laboratory, Institute for Solid State Physics, The University of Tokyo, Chiba, Japan and [2]Sumitomo Bakelite Co., Ltd., Hyogo, Japan
Correspondence: Y Shudo, Corporate R&D Center, Sumitomo Bakelite Co., Ltd., 1-1-5 Murotani, Nishi-ku, Kobe, Hyogo 651-2241, Japan.
E-mail: yshudo@sumibe.co.jp
or Professor M Shibayama, Neutron Science Laboratory, Institute for Solid State Physics, The University of Tokyo, 5-1-5 Kashiwanoha, Kashiwa, Chiba 277-8581, Japan.
E-mail: sibayama@issp.u-tokyo.ac.jp
Received 15 December 2014; revised 28 January 2015; accepted 28 January 2015; published online 18 March 2015

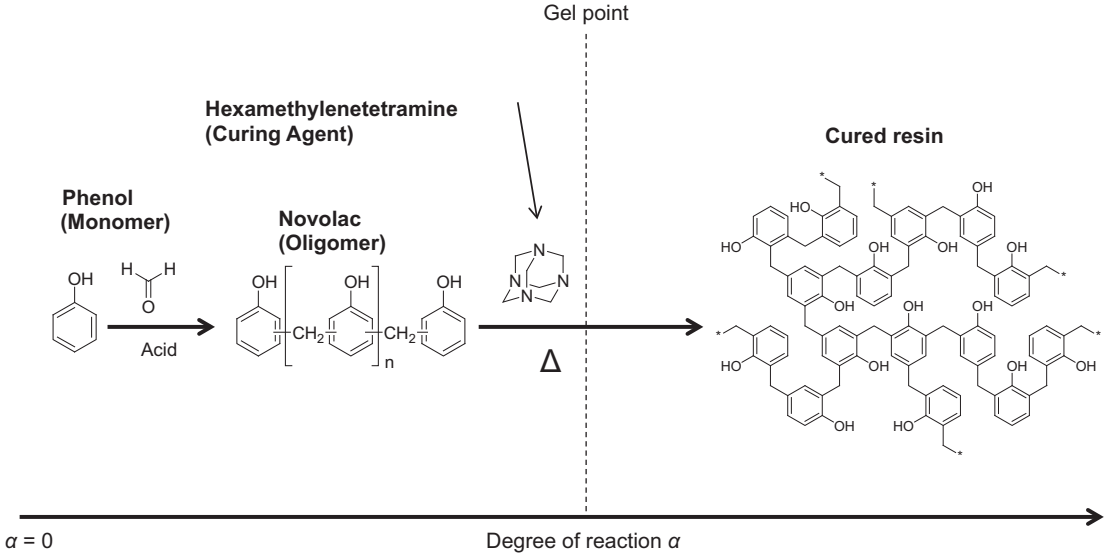

Figure 1 Schematic illustrations of the molecular structure of phenolic resins used in typical industrial applications. The degree of reaction (α) is defined as the fraction of reacted *ortho*- and *para*-positions that are adjacent to hydroxyl groups on the phenolic rings.

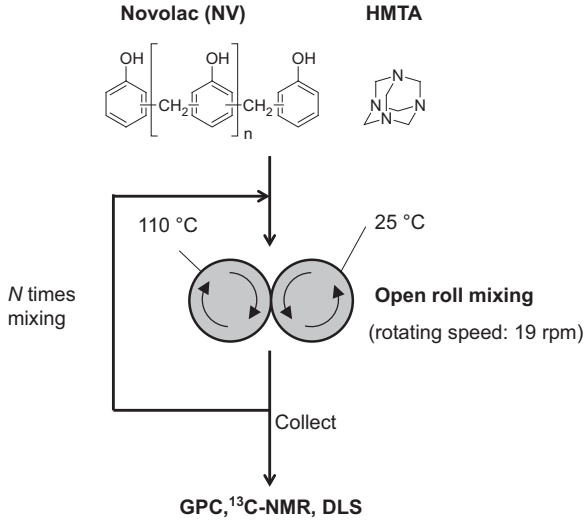

Figure 2 Sample preparation using an open two-roll mixing process. Aliquots of the reaction mixture were collected for GPC, ^{13}C NMR and DLS analyses.

investigation on the structural inhomogeneity of insoluble phenolic networks near the gel point, and highly cured networks reacted with HMTA.[18–20] Our previous study of the gelation mechanism using SAXS demonstrated that the scattering function of phenolic resins in a tetrahydrofuran (THF) solution or fully THF-swollen states can be described by a combination of the Ornstein–Zernike and squared Lorentzian equations, which have correlation lengths of several nanometers.[19,20] The change in correlation length during the gelation process indicates the presence of two different gelation mechanisms that are dependent on the amount of cross-linker. Our previous study of fully cured phenolic resins using SAXS and SANS indicated that the crosslinks were randomly distributed over the observed range (that is, 3–1600 nm). In addition, the spatial inhomogeneity of the crosslinks was very small and negligible compared with the inhomogeneity of voids with sizes ranging from tens to hundreds of nanometers. The existence of voids was elucidated through complementary SAXS and SANS analyses.[18]

Herein we report the evolution of NV clusters during the curing process in the pregel regime and the influence of an excess amount of HMTA on this evolution using DLS and gel permeation chromatography (GPC). An open two-roll mixing mill process was applied to control α by changing the number of roll-mixing times (N). The mechanical properties of the obtained phenolic resins that were prepared using varying amounts of HMTA after roll mixing and compression molding were also evaluated using a flexural test.

EXPERIMENTAL PROCEDURE

Materials

A novolac-type phenolic resin oligomer PR-53195 (NV) was provided by Sumitomo Bakelite Co., Ltd. (Tokyo, Japan), and HMTA (Figure 1) was purchased from Chang Chung Petrochemical Co., Ltd (Taipei, Taiwan). A random-type phenolic resin was synthesized using phenol, 37 wt% aqueous formaldehyde and oxalic acid. The number-average molecular weight (M_n) and M_w were determined to be 0.98×10^3 and 2.37×10^3 g mol^{-1}, respectively, using GPC. THF was purchased from Wako Pure Chemical Industries, Ltd (Osaka, Japan). Methanol-d_4 (99.9 at% D, containing 0.05 vol% tetramethylsilane) was purchased from C/D/N Isotopes, Inc (Pointe-Claire, Quebec, Canada). All of the materials were used as received without further purification. THF was used as the solvent for the GPC and DLS analyses, because it is a good solvent for NVs.

Sample preparation

The sample preparation procedures are shown in Figure 2. NVHX-16.7 and NVHX-15 were 1700/300 and 1700/225 (g/g) mixtures of NV and HMTA, respectively, and prepared by mechanical blending using a grinder-type mixer. The initial molar ratios of the methylene groups in the NV and HMTA and the phenolic rings in the NV ($[CH_2]_0/[PhOH]_0$) were 1.67 and 1.50, respectively, for NVHX-16.7 and NVHX-15, respectively. These ratios were estimated using the M_n of NV. $[CH_2]_0/[PhOH]_0 = 1.50$ corresponds to the stoichiometric ratio for NV. However, the NVHX-16.7 system contained an excess amount of HMTA. It is important to note that the ratio is within the range that is typically employed in industry.[2,3]

As shown in Figure 2, a two-roll mixing mill process was performed using an open 12-inch two-roll mixing mill (Toyo Sekkei Co., Ltd, Tokyo, Japan), which consists of two horizontally placed hollow metal rolls rotating toward each

other at the same speed (that is, 19 r.p.m.). The surface temperatures of the two rolls were set to 110 and 25 °C and controlled within a range of ± 1 °C during the mixing process. The mixing of NV and HMTA occurred in the melted state during the initial mixing stage because the melting temperature of NV was 80–90 °C. The two-roll mixing mill process was performed above the gel point until a THF-insoluble material was obtained, and the time interval was 40 s for the subsequent mixing procedure. During the two-roll mixing, small amounts of the reaction mixture were collected at different times and cooled to room temperature. The samples obtained below the gel point were used for GPC, ^{13}C NMR and DLS analyses. The number of mixing times (N) for each sample is listed in Table 1. THF-insoluble portions were obtained at $N = 130$ for NVHX-16.7 and $N = 135$ for NVHX-15.

GPC analyses

GPC experiments were performed using a Tosoh HLC-8320 system (Tosoh, Tokyo, Japan) equipped with four poly(styrene-*co*-divinylbenzene) gel columns (TSKgel SuperHZ-H, SuperHZ-H, SuperH2000, SuperH2000) and a Viscotek TDA302 system (Viscotek Corporation, Houston, TX, USA) equipped with a differential refractive index (RI) detector. The polymer concentration in each injection solution was 0.20 wt%, and the solutions were filtered through a 0.20-μm filter (Tosoh H-13-2) prior to injection. THF at 40 °C was used as the eluent. The results obtained with the RI detector were used along with a calibration curve generated using 14 polystyrene standards to calculate the M_w and M_n values for the polymers. The peak molecular weights of the polystyrene standards were 8.42×10^6, 5.48×10^6, 2.11×10^6, 7.06×10^5, 4.27×10^5, 1.90×10^5, 9.64×10^4, 3.79×10^4, 1.81×10^4, 1.02×10^4, 5.97×10^3, 2.42×10^3, 1.01×10^3 and 5.00×10^2 g mol^{-1}. The GPC results are listed in Table 1.

^{13}C NMR analyses

A JEOL JNM-ECA500 FT-NMR spectrometer (JEOL Ltd., Tokyo, Japan) operating at 500 MHz was used for ^{13}C NMR analyses. The ^{13}C NMR spectra were recorded using 10 000 scans at room temperature. A 10 wt% solution in methanol-d_4 was used for each measurement after filtering through a 0.20-μm filter (Tosoh H-13-2), which was also used for the GPC measurements. The α value was calculated according to a previous published protocol[10,27] using the signal intensities of the aromatic carbons observed at 110–160 p.p.m., and the results are listed in Table 1.

Dynamic light scattering

DLS were performed on a static/dynamic compact goniometer DLS/SLS-5000 (ALV, Langen, Germany). A He–Ne laser with a 22-mW emitting polarized light at a wavelength of 632.8 nm was used as the incident beam. DLS measurements were conducted at 25 °C with an acquisition time of 30 s. The scattering angle (θ) was 90°. The polymer concentration was 1.0 vol%, and each polymer solution was filtered through a 0.20-μm filter (Tosoh H-13-2), which was used for GPC analyses. The DLS results were used to calculate the time–intensity correlation function ($g^{(2)}(\tau)$) as a function of the decay time (τ) as follows:

$$g^{(2)}(\tau) = \frac{\langle I(\tau)I(0)\rangle}{\langle I(0)\rangle^2} = 1 + \left|g^{(1)}(\tau)\right|^2, \quad (1)$$

where $I(\tau)$ denotes the scattering intensity at time τ, $<\ldots>$ indicates the time average and $g^{(1)}(\tau)$ represents the scattering electric field intensity–time correlation function, which is described using a Laplace transform of the characteristic decay time distribution function ($G(\Gamma)$) and is given by:

$$g^{(1)}(\tau) = \int_0^\infty G(\Gamma)\exp(-\Gamma\tau)\mathrm{d}\Gamma, \quad (2)$$

where Γ is the characteristic decay rate. In the present study, the constrained regularization program CONTIN,[28] which is supplied with the correlator, was used to calculate $G(\Gamma)$ from $g^{(2)}(\tau)$. For dilute polymer solutions, Γ is related to the translational diffusion coefficient (D), which is given as follows:

$$\Gamma = Dq^2, \quad (3)$$

where q denotes the magnitude of the scattering vector ($\mathbf{q}$), which is defined by:

$$q = |\mathbf{q}| = \frac{4\pi n_0}{\lambda}\sin\frac{\theta}{2}, \quad (4)$$

where n_0 and λ denote the refractive index of the solvent and the wavelength of light in vacuum, respectively. Then, R_h of the polymer in the dilute solution is obtained using the Stokes–Einstein equation:

$$R_h = \frac{k_B T}{6\pi\eta D}, \quad (5)$$

where k_B, T and η are the Boltzmann constant, the absolute temperature and the solvent viscosity, respectively. The η and n_0 values for THF at 25 °C are 0.456 mPa s[29] and 1.404[30], respectively.

Flexural test

The mechanical properties of the phenolic resin were evaluated using an autograph AG-X 5kN (Shimadzu Corp., Kyoto, Japan). The flexural tests were performed according to the 178:2010 ISO standard. The NVHX-16.7 and NVHX-15 specimens for the flexural test were prepared by compression molding using a compression molding machine (Shinto Metal Industries Corp., Osaka, Japan). Granulated NVHX-16.7 and NVHX-15 were placed in a molding die and molded at 175 °C for 3 min under a pressure of 10 MPa, followed by curing at 180 °C for 6 h under atmospheric pressure. The approximate size of the test pieces were 10 mm × 4 mm × 80 mm. The NVHX-16.7 and NVHX-15 samples used for molding were obtained after two-roll mixing at $N = 125$ and 130, respectively. The three-point flexural test was performed three times to determine the flexural modulus and strength of each sample at 25 °C and atmospheric pressure. The obtained average and s.d. are provided in Table 2.

Table 1 Sample IDs and ^{13}C NMR and GPC results

Sample ID	N	α	$M_n/10^3$ g mol^{-1}	$M_w/10^3$ g mol^{-1}
NVHX-16.7	0	0.589	0.980	2.37
	90	0.590	1.21	3.26
	110	0.591	1.61	3.76
	120	0.624	1.74	3.97
	125	0.630	2.70	4.51
NVHX-15	0	0.589	0.980	2.37
	90	0.590	1.16	2.89
	110	0.593	1.82	3.23
	125	0.618	2.30	3.83
	130	0.628	3.02	4.34

Abbreviations: GPC, gel permeation chromatography; NMR, nuclear magnetic resonance.

RESULTS AND DISCUSSION

Figure 3 shows the GPC chromatograms for NVHX-16.7 after various mixing times, and the curves are normalized with respect to the total chromatogram area. The peaks located at retention times of 21.5, 20.3, 19.7 and 19.2 min correspond to the unreacted phenol monomer, dimer, trimer and tetramer, respectively. The intensities of these signals did not change significantly during the roll-mixing process. However, as the reaction proceeded, the intensities of the signals corresponding to 5000–10 000 and 1000–5000 g mol^{-1} increased at 15–16 min and decreased at 16–17 min, respectively. This behavior was also observed for NVHX-15. These results indicate that intermolecular reactions between larger molecules with molecular weights of 1000–5000 g mol^{-1} become dominant as the gel point is reached, and only a few low molecular weight components, such as the monomer, dimer and trimer, participated in the reactions. This behavior is in agreement with the gelation mechanism previously proposed for phenolic resins by Yamagishi *et al.*[31,32] based on Monte Carlo simulations of phenol–formaldehyde polycondensation

Table 2 Flexural modulus and strength of molded phenolic resins

Sample ID	*Flexural modulus/GPa*	*Flexural strength/MPa*
NVHX-16.7	6.2±0.0	120±20
NVHX-15	5.9±0.0	110±13

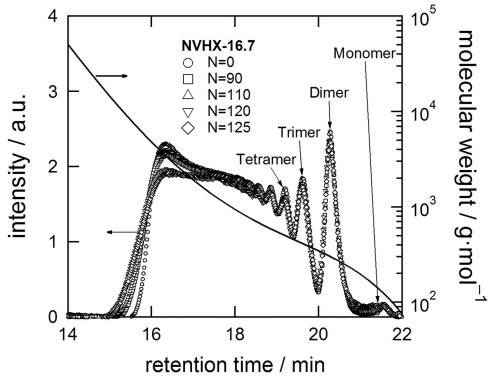

Figure 3 Gel permeation chromatograms of NVHX-16.7 measured in THF at 40 °C. The solid line represents the calibration curve based on polystyrene standards.

reactions. It is important to note that the mechanism of the curing reaction of NV with HMTA as the curing agent is different from that in the phenol–formaldehyde polycondensation reaction. However, this agreement indicates the general gelation behavior of phenolic resins. For further confirmation of this assumption, molecular dynamics simulations, including simulations of the cross-linking reaction,[15,33] are considered to be important. Statistical approaches that analyze the gelation kinetics, such as the cascade theory,[34,35] are also promising tools because they can be used to estimate molecular weight distributions with high precision.

Table 1 lists the α, M_w and M_n values for NVHX-16.7 and NVHX-15 after the two-roll mixing mill process. Gelation occurred at $N = 130$ and 135 for NVHX-16.7 and NVHX-15, respectively, and was defined as the moment when the THF-insoluble material was obtained. Figure 4 shows the M_w values for NVHX-16.7 and NVHX-15 as a function of N. Initially, the M_w values gradually increased with N and then sharply increased. In addition, the M_w values for NVHX-16.7 were larger than those of NVHX-15. These results indicate that, in the chemical reaction between the NV and HMTA, the amount of HMTA is rate limiting. This behavior involves a multistage reaction of HMTA, which consists of the decomposition of HMTA into an intermediate structure followed by a subsequent methylene linkage reaction.[2] Therefore, as a curing agent, HMTA has an effective functionality that is lower than the ideal value until the methylene linkage reaction occurs. The reaction of NV and HMTA proceeds more rapidly when a greater quantity of HMTA was used for NVHX-16.7 and NVHX-15.

The degree of reaction at the gel point (α_c) was estimated to be 0.63 for both resins. As previously mentioned, α is defined as the conversion of reactive sites on phenol based on classical gelation theory in this study. Drumm and Leblanc[5] reported α_c values of 0.763 for an initial formaldehyde/phenol molar ratio ($[CH_2]_0/[PhOH]_0$) of 0.60–0.85 using classical gelation theory and the average molecular weights.[5–7] Yamagishi *et al.*[31,32] reported an α_c value of 0.78 for a $[CH_2]_0/[PhOH]_0$ ratio of 1.2 using Monte Carlo simulations for a gelation model. Izumi *et al.*[16] reported α_c values of 0.620, 0.647 and 0.680 for $[CH_2]_0/[PhOH]_0$ ratios of 1.0, 1.2 and 1.5, respectively, using rate equations derived by Aranguren *et al.*[36] to investigate the reaction kinetics. The α_c value of 0.63 obtained from the novolac/HMTA reaction is within the range of these reported values.

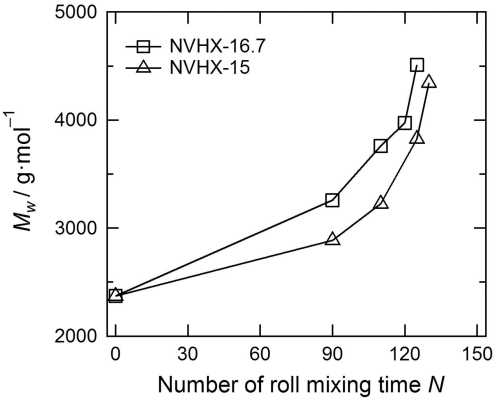

Figure 4 Changes in the weight-average molecular weights of NVHX-16.7 and NVHX-15 during open two-roll mixing.

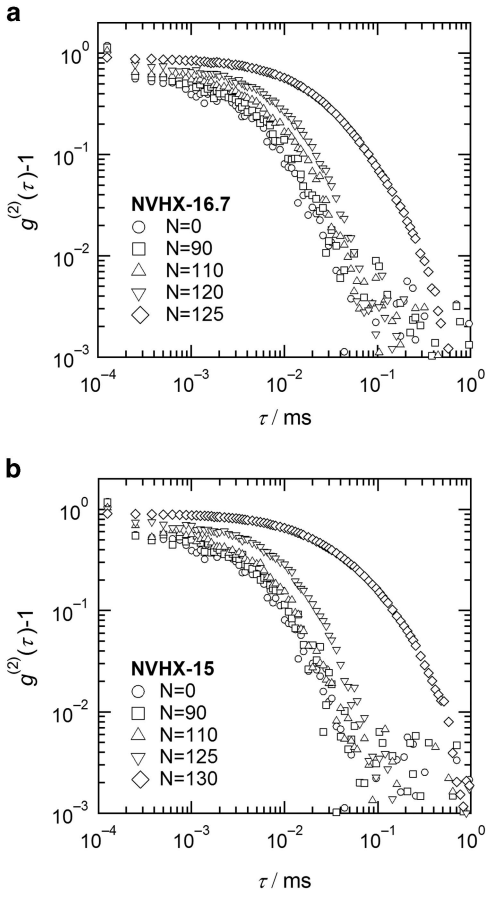

Figure 5 Time–intensity correlation functions of (**a**) NVHX-16.7 and (**b**) NVHX-15 in THF at 25 °C.

Figure 5 shows the changes in the $g^{(2)}(\tau)$ values for NVHX-16.7 and NVHX-15 as a function of N. The correlation function shifted toward a longer relaxation time as the reaction proceeded, which indicates an increase in the average molecular size due to the roll-mixing process. The $G(\Gamma)$ distribution functions of R_h in THF are shown in Figure 6. The shift in the distribution functions toward larger sizes indicates an increase in the molecular sizes. Interestingly, as the gel point is

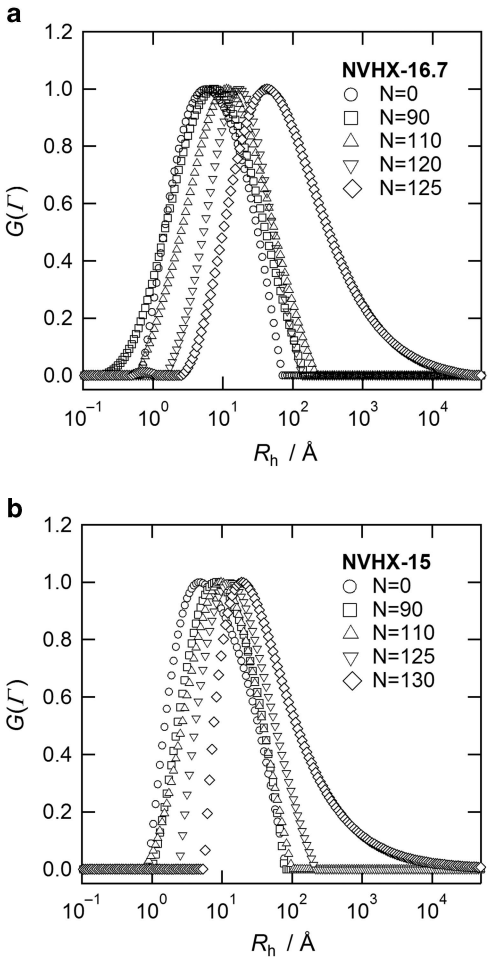

Figure 6 Distribution functions for the hydrodynamic radius of (**a**) NVHX-16.7 and (**b**) NVHX-15 in THF at 25 °C.

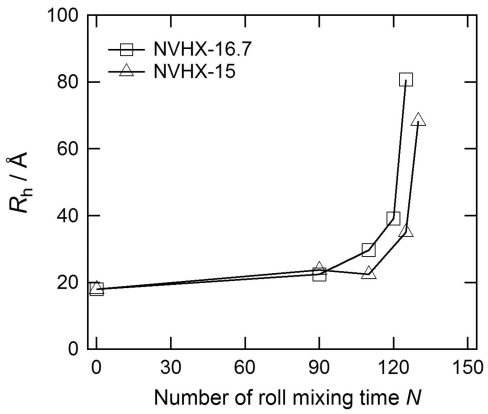

Figure 7 Changes in the hydrodynamic radius R_h of NVHX-16.7 and NVHX-15 during the open two-roll mixing process.

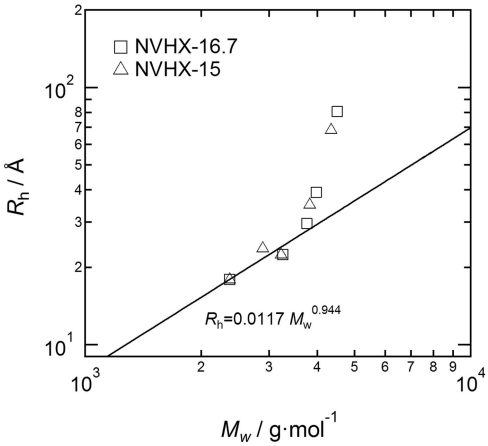

Figure 8 Hydrodynamic radius (R_h) as a function of the weight-average molecular weight (M_w). The solid line is the fitted result in a M_w range of 2000–4000 g mol^{-1}.

reached, significant changes in the distributions of both NVHX-16.7 and NVHX-15 are observed. Therefore, the order of magnitude of the right tail of the distribution increases from 10^2 ($N=125$) to 10^4 Å ($N=130$) during the last five mixing procedures. These results also support the conclusion that reactions between larger molecules become dominant as the gel point is reached.

Figure 7 shows the changes in R_h (determined from Γ at the point of maximum $G(\Gamma)$) for NVHX-16.7 and NVHX-15 as a function of N. An increase in R_h was observed for both systems as the roll mixing proceeded even though NVHX-16.7 grew faster and its molecular weight was greater than that of NVHX-15. In addition, a remarkable increase in R_h was observed in the vicinity of the gel point for both NVHX-16.7 and NVHX-15. Therefore, the dependence of R_h on the molecular weight was studied to further investigate this behavior.

Figure 8 shows a plot of R_h as a function of M_w, where R_h and M_w exhibited a power-law behavior with an exponent value of 0.944 in a M_w range of 2000–3800 g mol^{-1}, which agrees with the previously reported value of 0.948 for phenolic resins prepared via by phenol–formaldehyde polycondensation.[16] However, a deviation from the power-law relationship was observed in a M_w range >4000 g mol^{-1}. This change in the relationship may be due to an overestimation of the R_h values due to the formation of larger molecules as the gel point is reached. As previously discussed,[16] the scattering intensity from large molecules should be dominant in the DLS results because the intensity is proportional to the sixth power of the size of the scatterer. In addition, it is difficult to estimate the average value of R_h for polymers with a broad molecular weight distribution, which has been observed for phenolic resins.[24]

The distinct increase in R_h and the deviation from the power-law relationship as the gel point is reached may also be explained by the previously proposed curing mechanism for NV with HMTA, which involved a change in the mechanism during curing.[2,9,12,37,38] In particular, Zhang *et al.*[9] investigated the curing mechanism using ^{13}C and ^{15}N NMR and reported that the decomposition of HMTA resulted in a decrease in the pH of the system. Because NV and HMTA are acidic and basic compounds, respectively, the decrease in the pH further accelerated the decomposition of HMTA and the formation of methylene cross-linkers.[9] In addition, hydrogen bond-stabilized benzoxazine and benzylamine were the major initial intermediates generated in the cross-linking reaction, and their decomposition resulted in cross-linking reactions via methylene linkages. A change in the reaction mechanism during the curing process was also reported by de Medeiros *et al.*[12] based on kinetic analysis using the dynamic Ozawa method and differential scanning calorimetry. Therefore, the initial power-law relationship may correspond to chain growth of the NV resin along with the formation of intermediates, and the distinct increase in R_h and deviation from the

power-law relationship may be due to cross-linking via methylene linkages, following the decomposition of the intermediates. In addition, these results indicate that, based on the solution conformation, a large excess amount of HMTA does not affect the curing mechanism of NV below the gel point.

The values for the flexural modulus and strength of NVHX-16.7 and NVHX-15 after compression molding are shown in Table 2. NVHX-16.7 exhibits a higher modulus and strength compared with NVHX-15. However, there is no significant difference in the R_h–M_w relationship for the two resins. Therefore, the structural differences governing the mechanical properties are determined by the ratio of NV to HMTA (Figure 4) and formed after the gelation process. This result suggests that the curing mechanism is similar to that of the phenol–formaldehyde gelation systems.[19,20] The different rates observed for the R_h and M_w growth curves as a function of N for the resin systems with different NV/HMTA ratios should be expressed as the structural differences in the cross-linked structures after gelation. Because it is difficult to apply DLS analysis in the postgel regime due to coloration and low transparency, SAXS and SANS analyses are indispensable tools for further structural analysis of the NV/HMTA reaction mixtures above the gel point.[18–20]

It is important to note that this study demonstrated the successful application of the open two-roll mixing mill to control the degree of reaction for the curing of NV with HMTA by varying the number of roll-mixing times (N). By controlling the degree of reaction, it was possible to investigate the critical behavior of the NV/HMTA system near the gel point.

CONCLUSION

The behavior of the NV cured with HMTA in the pregel regime and the influence of an excess amount of HMTA on the curing reaction were investigated using DLS. A two-roll mixing mill process was applied to control the degree of reaction. The growth rates for the molecular weight and hydrodynamic radius of NV as a function of the number of mixing times were very different and dependent on the amount of HMTA. A plot of the hydrodynamic radius of NV in THF as a function of M_w indicated two different growth mechanisms during NV curing with HMTA in the pregel regime irrespective of the amount of HMTA. An initial power-law relationship with a scaling exponent of 0.94 and a subsequent large deviation from this relationship were observed. As the gel point was reached, intermolecular reactions between larger molecules became dominant due to cross-linking via methylene linkages, which occurred after the decomposition of the initially formed HMTA decomposition products.

These results suggest that the structural differences governing the mechanical properties of phenolic resins are established in the pregel stage followed by noticeable differences in the mechanical properties during the subsequent curing process. To further elucidate the curing mechanism, SAXS and SANS analyses of the gelation process,[18–20] atomistic molecular dynamics simulations of cross-linked network structures[15,33] and refinement of the gelation kinetics using statistical approaches, such as the cascade theory,[34,35] are promising methods.

1 Baekeland, L. H. Method of making insoluble products of phenol and formaldehyde, USA, Patent 942699 (1907).
2 Gardziella, A., Pilato, L. A. & Knop, A. *Phenolic Resins: Chemistry, Applications, Standardization, Safety and Ecology* 2nd edn (Springer, Berlin, Germany, 1999).
3 Pilato, L. *Phenolic Resins: A Century of Progress* (Springer, Berlin, Germany, 2010).
4 Pascault, J. P., Sautereau, H., Verdu, J. & Williams, R. J. J. *Thermosetting Polymers* (Marcel Dekker, New York, NY, USA, 2002).
5 Drumm, M. F. & Leblanc, J. R. *Step Growth Polymerizations* Vol. 3 (ed. Solomon, D. H.) Ch. 5, 157–278 (Marcel Dekker, New York, NY, USA, 1972).
6 Borrajo, J., Aranguren, M. I. & Williams, R. J. J. Statistical aspects for the production of novolacs. *Polymer* **23**, 263–266 (1982).
7 Stockmayer, W.H. Theory of Molecular Size Distribution and Gel Formation in Branched-Chain Polymers. *J. Chem. Phys.* **11**, 45–55 (1943).
8 Carotenuto, G. & Nicolais, L. Kinetic study of phenolic resin cure by IR spectroscopy. *J. Appl. Polym. Sci.* **74**, 2703–2715 (1999).
9 Zhang, X., Looney, M. G., Solomon, D. H. & Whittaker, A. K. The chemistry of novolac resins: 3. ^{13}C and ^{15}N n.m.r. studies of curing with hexamethylenetetramine. *Polymer* **38**, 5835–5848 (1997).
10 Sojka, S. A., Wolfe, R. A. & Guenther, G. D. Formation of phenolic resins: mechanism and time dependence of the reaction of phenol and hexamethylenetetramine as studied by carbon-13 nuclear magnetic resonance and fourier transform infrared spectroscopy. *Macromolecules* **14**, 1539–1543 (1981).
11 Nomoto, M., Fujikawa, Y., Komoto, T. & Yamanobe, T. Structure and curing mechanism of high-ortho and random novolac resins as studied by NMR. *J. Mol. Struct.* **976**, 419–426 (2010).
12 de Medeiros, E. S., Agnelli, J. A. M., Joseph, K., de Carvalho, L. H. & Mattoso, L. H. C. Curing behavior of a novolac-type phenolic resin analyzed by differential scanning calorimetry. *J. Appl. Polym. Sci.* **90**, 1678–1682 (2003).
13 Dominguez, J. C., Alonso, M. V., Oliet, M., Rojo, E. & Rodriguez, F. Kinetic study of a phenolic-novolac resin curing process by rheological and DSC analysis. *Thermochim. Acta* **498**, 39–44 (2010).
14 Markovic, S., Dunjic, B., Zlatanic, A. & Djonlagic, J. Dynamic mechanical analysis study of the curing of phenol-formaldehyde novolac resins. *J. Appl. Polym. Sci.* **81**, 1902–1913 (2001).
15 Izumi, A., Nakao, T. & Shibayama, M. Atomistic molecular dynamics study of cross-linked phenolic resins. *Soft Matter* **8**, 5283–5293 (2012).
16 Izumi, A., Takeuchi, T., Nakao, T. & Shibayama, M. Dynamic light scattering and small-angle neutron scattering studies on phenolic resin solutions. *Polymer* **52**, 4355–4361 (2011).
17 Izumi, A., Nakao, T. & Shibayama, M. Synthesis and properties of a deuterated phenolic resin. *J. Polym. Sci. A Polym. Chem.* **49**, 4941–4947 (2011).
18 Izumi, A., Nakao, T., Iwase, H. & Shibayama, M. Structural analysis of cured phenolic resins using complementary small-angle neutron and X-ray scattering and scanning electron microscopy. *Soft Matter* **8**, 8438–8445 (2012).
19 Izumi, A., Nakao, T. & Shibayama, M. Gelation and cross-link inhomogeneity of phenolic resins studied by ^{13}C-NMR spectroscopy and small-angle X-ray scattering. *Soft Matter* **9**, 4188–4197 (2013).
20 Izumi, A., Nakao, T. & Shibayama, M. Gelation and cross-link inhomogeneity of phenolic resins studied by small- and wide-angle X-ray scattering and ^{1}H-pulse NMR spectroscopy. *Polymer* **59**, 226–233 (2015).
21 Shibayama, M. Spatial inhomogeneity and dynamic fluctuations of polymer gels. *Macromol. Chem. Phys.* **199**, 1–30 (1998).
22 Shibayama, M. & Norisuye, T. Gel formation analyses by dynamic light scattering. *Bull. Chem. Soc. Jpn* **75**, 641–659 (2002).
23 Shibayama, M., Ozeki, S. & Norisuye, T. Real-time dynamic light scattering on gelation and vitrification. *Polymer* **46**, 2381–2388 (2005).
24 Shibayama, M., Karino, T. & Okabe, S. Distribution analyses of multi-modal dynamic light scattering data. *Polymer* **47**, 6446–6456 (2006).
25 Chen, W., Wu, J. & Jiang, M. Phase separation in hexamethylenetetramine cross-linked Novolac/poly(ethylene-co-vinyl acetate) blends. *Polymer* **39**, 2867–2874 (1998).
26 Yoonessi, M., Toghiani, H., Wheeler, R., Porcar, L., Kline, S. & Pittman, C. U. Jr. Neutron scattering, electron microscopy and dynamic mechanical studies of carbon nanofiber/phenolic resin composites. *Carbon* **46**, 577–588 (2008).
27 Nomoto, M., Yamagishi, T. & Nakamoto, Y. Determination of branch density for high-ortho novolac and random novolac using ^{13}C-NMR. *J. Network Polym. Jpn* **27**, 210–217 (2006).
28 Provencher, S. W. A constrained regularization method for inverting data represented by linear algebraic or integral equations. *Comput. Phys. Commun.* **27**, 213–227 (1982).
29 Yaws, C. L. *Handbook of Viscosity* (Gulf Professional Publishing, Houston, TX, USA, 1995).
30 Wohlfarth, C. & Wohlfarth, B. *Optical Constants: Subvolume B: Refractive Indices of Organic Liquids* (ed. Lechner M. D.) (Springer, Berlin, Germany, 1996).
31 Yamagishi, T., Nakatogawa, T., Ikuji, M., Nakamoto, Y. & Ishida, S. Computational study of network formation of phenolic resins. *Angew. Makromol. Chem.* **240**, 181–186 (1996).
32 Yamagishi, T., Nakamoto, Y. & Ishida, S. Gelation reaction of phenolic resins. *Kobunshi Kako Jpn.* **34**, 178–183 (1999).
33 Yarovsky, I. & Evans, E. Computer simulation of structure and properties of crosslinked polymers: application to epoxy resins. *Polymer* **43**, 963–969 (2002).
34 Nakao, T., Tanaka, F. & Kohjiya, S. Cascade theory of substitution effects in nonequilibrium polycondensation systems. *Macromolecules* **35**, 5649–5656 (2002).
35 Nakao, T., Tanaka, F. & Kohjiya, S. New cascade theory of branched polymers and its application to size exclusion chromatography. *Macromolecules* **39**, 6643–6652 (2006).
36 Aranguren, M. I., Borrajo, J. & Williams, R. J. J. Statistics of novolacs. *Ind. Eng. Chem. Prod. Res. Dev.* **23**, 370–374 (1984).
37 Katovic, Z. & Stefanic, M. Intermolecular hydrogen bonding in novolacs. *Ind. Eng. Chem. Prod. Res. Dev.* **2**, 179–185 (1985).
38 Looney, M. G. & Solomon, D. H. The chemistry of novolac resins. I. A review on the use of models. *Aust. J. Chem.* **48**, 323–331 (1995).